Journal of Thermal Analysis and Calorimetry, Vol. 63 (2001) 59–68

THE REACTIVITY OF MANGANITES IN ^{18}O ISOTOPE EXCHANGE REACTIONS

I. A. Koudriashov[1], *G. N. Mazo*[1], *I. K. Murwani*[2], *S. Scheurell*[2] *and E. Kemnitz*[2]

[1]Moscow State University, Department of Inorganic Chemistry, 11899 Moscow, Russia
[2]Institut für Chemie, Humboldt-Universität zu Berlin, Hessische Str. 1/2, 10115 Berlin, Germany

(Received May 7, 2000)

Abstract

The effect of the structural properties and the oxidation state of Mn on the ^{18}O isotope exchange behaviour of ternary manganites ($La_{1-x}Sr_xMnO_3$, $La_{0.5}Sr_{1.5}MnO_4$ and $SrMnO_3$) has been studied. All types of ^{18}O isotope exchange (homomolecular, partially and completely heteromolecular) take place on the very active manganites with perovskite ($LaMnO_3$ and $La_{0.7}Sr_{0.3}MnO_3$) and perovskite-like ($SrMnO_3$) structure, but not on the less active K_2NiF_4-structure ($La_{0.5}Sr_{1.5}MnO_4$). The highest ^{18}O exchange activity is observed for $La_{0.7}Sr_{0.3}MnO_3$, for which the completely heteromolecular ^{18}O exchange starts to occur at 520 K, already, a T_{on} which is typical for excellent redox catalysts. The influence of the structural properties on the ^{18}O exchange and oxygen diffusion behaviour of the manganites is much more pronounced than that of the Mn^{3+}/Mn^{4+} ratio. The different reduction behaviour of the manganites with perovskite and K_2NiF_4-structure can be explained by means of the bond-valence model.

Keywords: CH_4 oxidation, CO oxidation mechanism, ^{18}O isotope exchange, ternary manganites

Introduction

Perovskite-like oxides of 3d-transition elements with highly disordered structure [1] are promising objects for elaboration of multi-functional materials. Among such oxides, manganites $(La,Sr)MnO_{3+\delta}$ and $(La,Sr)_{n+1}Mn_nO_{3n+1}$ (n=1, 2) attracted considerable attention due to their peculiar physical properties (e.g. giant magneto resistance [2, 3]) and catalytic activity [4–9]. Therefore, some effort has been made to study the activity of perovskite-like manganites ($La_{1-x}Sr_xMnO_3$, x=0–0.5) in isotope exchange [10, 11] and oxidation reactions [4–9]. According to Sazanov *et al*. [10], the activation energy of the homomolecular exchange of oxygen ($^{16}O_{2(g)}+{}^{18}O_{2(g)}=2{}^{16}O{}^{18}O_{(g)}$) on $LaMnO_3$ at T>573 K is about 20 kcal mol^{-1}. The perovskite-like manganites catalyze the carbon monoxide oxidation at T=373–673 K [4–6] and the methane oxidation at T=623–873 K [7–9]. Two opposite trends are observed investigating the effect of Sr substitution for La on methane oxidation at various temperatures [7]. At

1418–2874/2001/ $ 5.00

Akadémiai Kiadó, Budapest
Kluwer Academic Publishers, Dordrecht

T<673 K the catalytic activity of the manganites increased with the degree of Sr substitution, i.e. $La_{0.6}Sr_{0.4}MnO_3$>$La_{0.8}Sr_{0.2}MnO_3$>$LaMnO_3$, while at higher temperatures (T>673 K) the order is reverse: $LaMnO_3$>$La_{0.8}Sr_{0.2}MnO_3$>$La_{0.6}Sr_{0.4}MnO_3$. The opposite behaviour is explained by two different factors affecting the catalytic activity. At lower temperatures, the activity is mainly determined by the concentration of anion vacancies on the surface that reaches its maximum value for $La_{0.6}Sr_{0.4}MnO_3$. However, as the temperature increases, the catalytic activity is controlled by the excess oxygen in the structures.

Usually, in catalytic studies less attention is paid to the influence of structural features and Mn^{3+}/Mn^{4+} ratio on the ^{18}O exchange behaviour and redox activity of manganites. The presence of vacancies, as well as the possibility to change the oxidation state of manganese may cause high oxygen mobility and activity in catalytic oxidation processes. For that reason, the ^{18}O exchange behaviour of the perovskites $LaMnO_3$ and $La_{0.7}Sr_{0.3}MnO_3$ was compared to that of the rarely considered $SrMnO_3$ (hexagonal perovskite-like structure) and $La_{0.5}Sr_{1.5}MnO_4$ (K_2NiF_4-structure). From the results, conclusions can be drawn on the oxidation activity of the manganites depending on their structure, vacancy concentration and Mn^{3+}/Mn^{4+} oxidation.

Experimental

Single-phase samples of $La_{1-x}Sr_xMnO_3$ (x=0; 0.3), $SrMnO_3$, $La_{0.5}Sr_{1.5}MnO_4$ were prepared using the conventional freeze-drying technique [6]. Metal nitrate solutions of well-defined concentration were mixed in an appropriate ratio and introduced into liquid nitrogen. The frozen mixture was transferred into a conventional freeze-drying machine (SMH-15, Usifroid) and dried in vacuum (p=5 Pa) to produce a highly homogeneous mixed nitrate precursor. The nitrate mixture was slowly heated to 773 K (heating rate 0.5 K min^{-1}) and calcinated for 20 h. After calcination, the powders were ground and annealed at temperatures between 873 and 1323 K in several steps for up to 80 h.

Phase composition and structure of the samples were analyzed by powder X-ray diffraction analysis using a Gunier-camera ($CuK_{\alpha 1}$-radiation, λ=1.54056 Å) with Ge as internal standard. A iodometric titration technique was employed for determining the Mn(IV):Mn(III) ratio in the manganite phases [12]. The BET-surface area of the samples was determined after degassing the powders at 573 K by analyzing the N_2 adsorption behaviour at liquid nitrogen temperature (ASAP 2100 system, Micromeritics). The average size of particles was measured by SEM a microscope JEM-2000FXII (U=200 kV).

The ^{18}O isotope exchange measurements were carried out in a quartz reactor with an on-line-coupled mass spectrometer. Before starting the reaction, the samples were heated for 4 h at 673 K in $^{16}O_2$ (p=200 Pa) in order to remove H_2O, CO_2 and other molecules from the surface of the oxide. After cooling down to 373 K, Ar and $^{18}O_2$ were introduced into the reaction system to adjust an initial pressure of 150 Pa (20 Pa Ar, 65 Pa $^{16}O_2$ and 65 Pa $^{18}O_2$). Subsequently, the quartz reactor was heated to 973 K applying a constant heating rate of 10 K min^{-1}. The variation of the gas phase composition during constant heating was analyzed by a quadropole mass spectrome-

ter QMG4211 (Pfeiffer Vacuum GmbH). During the interaction between $^{18}O_2$, $^{16}O_2$ and the solid oxide, diffusion, sorption, and ^{18}O isotope exchange (Eqs (1–3)) processes may take place.

Homomolecular ^{18}O isotope exchange

$$^{18}O_{2(g)} + {}^{16}O_{2(g)} \rightarrow 2{}^{16}O{}^{18}O_{(g)} \tag{1}$$

Partially heteromolecular ^{18}O isotope exchange

$$^{18}O_{2(g)} + {}^{16}O_{(s)} \rightarrow {}^{16}O{}^{18}O_{(g)} + {}^{18}O_{(s)} \tag{2a}$$

$$^{16}O{}^{18}O_{(g)} + {}^{16}O_{(s)} \rightarrow {}^{16}O_{2(g)} + {}^{18}O_{(s)} \tag{2b}$$

Completely heteromolecular ^{18}O isotope exchange

$$^{18}O_{2(g)} + 2{}^{16}O_{(s)} \rightarrow {}^{16}O_{2(g)} + 2{}^{18}O_{(s)} \tag{3}$$

These processes may take place separately or simultaneously, depending on the nature of the investigated compound and/or temperature. As far the isotope exchange between an oxide containing ^{16}O and a gas phase containing ^{18}O is accompanied by change of oxygen molecular forms in the gas phase, it is required to introduce the following coefficients in order to distinguish between the individual, simultaneously occurring processes [13, 14].

$$s = \frac{\{[^{16}O_2] + [^{16}O^{18}O] + [^{18}O_2]\}_{t=i}}{\{[^{16}O_2] + [^{16}O^{18}O] + [^{18}O_2]\}_{t=0}} = \frac{p_i}{p_0} \tag{4}$$

$$c = \frac{\frac{[^{16}O^{18}O]}{2} + [^{18}O_2]}{[^{16}O_2] + [^{16}O^{18}O] + [^{18}O_2]} \tag{5}$$

$$y = [^{16}O^{18}O]_{eq} - [^{16}O^{18}O]_{t=i} = 0.5 - \left(\frac{[^{16}O^{18}O]_{eq}}{[^{16}O_2] + [^{16}O^{18}O]_{eq} + [^{18}O_2]} \right) \tag{6}$$

$$\nu = \left(\frac{\frac{[^{16}O^{18}O]}{2}}{\frac{[^{16}O^{18}O]}{2} + [^{18}O_2]} \right)_{t=i} \left(\frac{\frac{[^{16}O^{18}O]}{2} + [^{18}O_2]}{\frac{[^{16}O^{18}O]}{2}} \right)_{t=0} \tag{7}$$

From the occurrence of the individual processes and the onset-temperatures, conclusions can be drawn on temperature regions of enhanced oxygen mobility and activity to promote homogeneous or heterogeneous redox reactions. The measuring principle and the theoretical background of the ^{18}O isotope exchange measurements were described in [15–18].

The bond-valence method was employed for calculating the parameter V_i that allows estimating the strength of oxygen chemical bonding for different manganite structures ($LaMnO_3$, $SrMnO_3$, and $La_{0.5}Sr_{1.5}MnO_4$) according to the following equation:

$$V_i = \sum_j s_{ij} = \sum_j \exp\left(\frac{r_0 - r_{ij}}{B}\right) \quad (8)$$

where B, r_0, r_{ij} were taken from [19].

Results and discussion

$LaMnO_3$, $La_{0.7}Sr_{0.3}MnO_3$ and $SrMnO_3$ were already formed at 773 K, the decomposition temperature of the freeze-dried precursor. At an annealing temperature of 873 and 973 K, large amounts of amorphous by-products were obtained, while single-phase perovskites were obtained at T=1073 K, only. The formation of $La_{0.5}Sr_{1.5}MnO_4$ starts to occur at 973 K, but a temperature of 1323 K was required to obtain the single-phase oxide without amorphous impurities.

Table 1 Structural parameters, average oxidation state of Mn, specific surface area and average grain size of manganite samples

Composition	Structural parameters			Z_{Mn}	S_{BET}/ $m^2\ g^{-1}$	Grain size/ nm
	Symmetry	a/Å	c/Å			
$LaMnO_{3.10}$	rhombohedral	5.5192(6)	13.330(2)	3.20	2.57	250
$La_{0.7}Sr_{0.3}MnO_{3.01}$	rhombohedral	5.5094(8)	13.367(3)	3.32	7.37	150
$La_{0.5}Sr_{1.5}MnO_{3.99}$	tetragonal	3.8587(9)	12.408(3)	3.47	1.72	350
$SrMnO_{2.96}$	hexagonal	5.4466(8)	9.072(2)	3.93	3.00	250

Table 1 summarizes the results of XRD, BET, and iodometric analysis. Although the average valence of Mn increases with the degree of substitution of Sr^{2+} for La^{3+}, the numerical excess oxygen content of the samples decreases. It has to be pointed out, however, that there is no real position for excess oxygen anions in the different structures. In $LaMnO_{3+\delta}$, the Mn^{4+} content is due to cation vacancies in the lattice [20–23]. In $La_{0.7}Sr_{0.3}MnO_3$, the Mn^{4+} content corresponds to the degree of substitution of Sr^{2+} for La^{3+}. Neither in $La_{0.5}Sr_{1.5}MnO_4$ nor in $SrMnO_3$, excess oxygen is expected. According to the results of iodometric analysis, $LaMnO_{3.10}$ is the only sample with a numerical excess of O^{2-} anions. The reduction of Mn^{4+} in $LaMnO_{3.10}$ is accompanied by phase transitions finally leading to a monoclinic symmetry of $LaMnO_{3.00}$ [20–23].

The results of specific surface area measurements were in fair agreement with those obtained from SEM (Fig. 1 and Table 1). The lower the grain size of the manganites is, the larger the BET-surface area is. The average grain size varied between 150 nm for $La_{0.7}Sr_{0.3}MnO_{3.01}$ and 350 nm for $La_{0.5}Sr_{1.5}MnO_{3.99}$. Due to the high annealing temperatures required for preparing single phases, the BET-surface area of the samples did not exceed 7.5 $m^2\ g^{-1}$, which is relatively low in comparison to Johnson *et al*. [6]. The present study, however, is aimed at analyzing the ^{18}O exchange behaviour

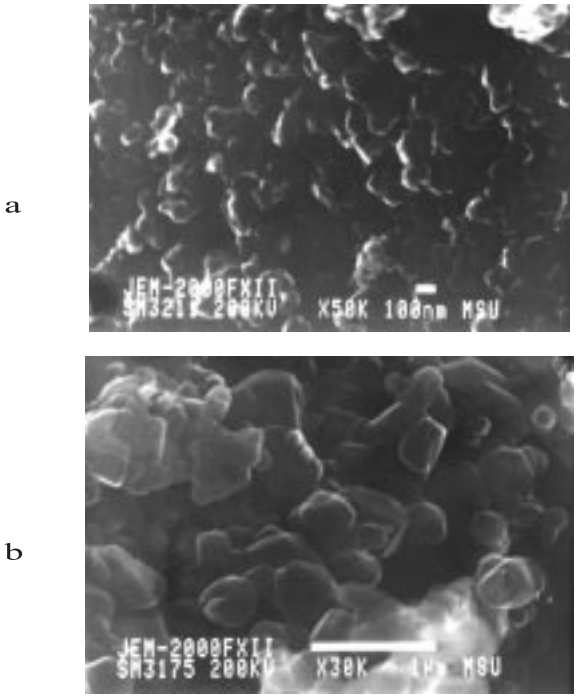

Fig. 1 SEM photograph of a – $La_{0.7}Sr_{0.3}MnO_3$ sample (×50000) and b – $La_{0.5}Sr_{1.5}MnO_4$ sample (×30000)

of manganites depending on structural but not on surface properties. Therefore, only samples without amorphous background in X-ray diffractograms were selected for polythermal ^{18}O exchange experiments and the sample mass was varied in such a way that the total surface area was constant.

Except for the slightly different $La_{0.5}Sr_{1.5}MnO_4$, the diffusion and ^{18}O isotope exchange of manganites with different structure is more or less similar. Therefore, the order of processes occurring during the constant heating of the manganites in an equimolar $^{16}O_2$:$^{18}O_2$ gas mixture can be exemplified on $LaMnO_{3.10}$ (Fig. 2). Up to 535 K, neither diffusion nor exchange processes take place. Above 535 K, $^{18}O_2$ is converted to $^{16}O_2$ by completely heteromolecular exchange (Eq. (3)). Constant coefficients *s, y*, and *v* indicate that the completely heteromolecular exchange is the only process between 535 and 575 K. At 575 K, $^{16}O^{18}O$ appears accompanied by the corresponding variation of the coefficients *v* and *y* ($v\uparrow$ and $y\downarrow$). Due to the simultaneous occurrence of the completely heteromolecular exchange ($c\downarrow$, y=const.), however, it cannot be unambiguously derived from Fig. 2, whether $^{16}O^{18}O$ is formed by homomolecular (Eq. (1)) or by partially heteromolecular exchange (Eq. (2a)). Two scenarios can explain the observed variation of the oxygen isotope distribution between 575 and 725 K, (i) by dominating completely heteromolecular and slow homomolecular ^{18}O exchange or by (ii) simultaneously occurring completely and partially heteromole-

cular ^{18}O exchange. At 725 K, the $^{16}O_2$ partial pressure stops increasing and remains almost constant up to 830 K. Since in-diffusion and adsorption can be excluded below 830 K (*s*=constant), the quasi-constant $^{16}O_2$ content between 725 and 830 K can only be explained by the simultaneous occurrence of homomolecular ^{18}O isotope exchange. The quantity $^{16}O_2$ formed by completely heteromolecular exchange (Eq. (3)) is immediately consumed by homomolecular exchange (Eq. (1)).

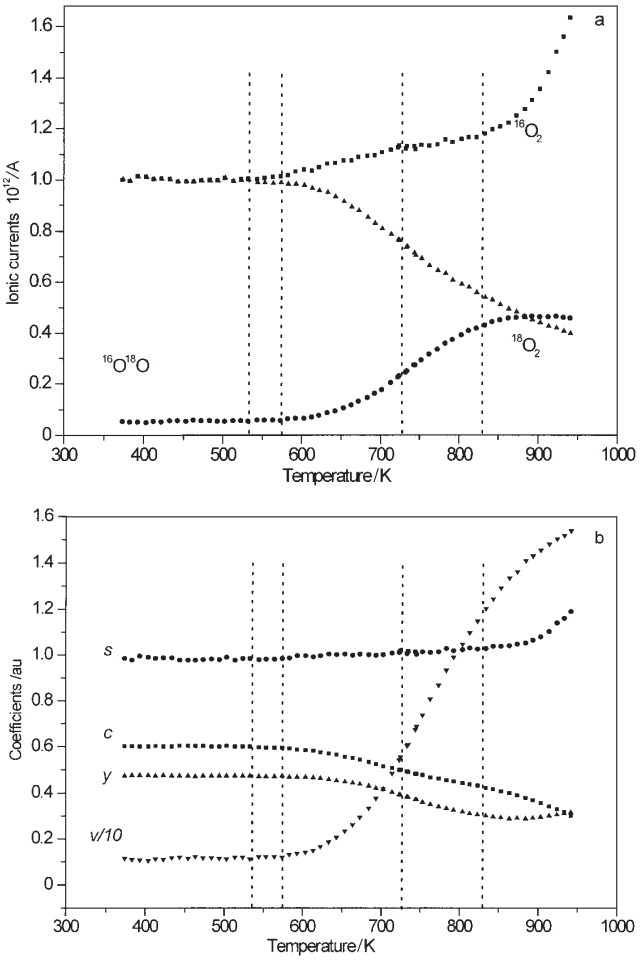

Fig. 2 Oxygen isotope distribution (a) and variation of coefficients (b), characterizing the ^{18}O exchange and diffusion behaviour of $LaMnO_{3.10}$ (p_0=150 Pa, heating rate 10 K min^{-1})

Apparently, in the 3rd temperature range, all the three ^{18}O exchange processes take place with different exchange rates. Consequently, the $^{18}O_2$ partial pressure decreases and $^{16}O^{18}O$ is increasingly converted to $^{16}O_2$ according to Eq. (2b). From the kinetic point of view, this reaction has to be considered as a partially heteromolecular exchange reaction

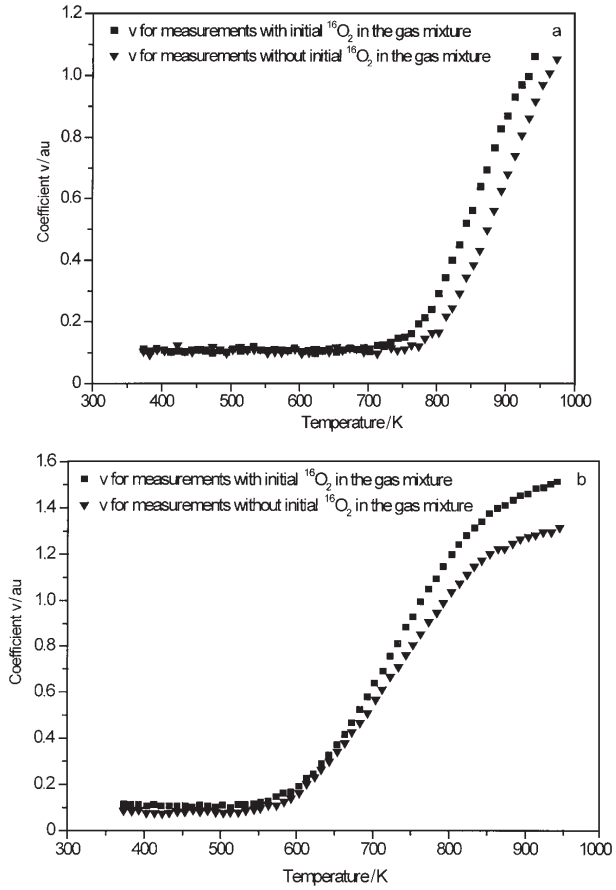

Fig. 3 Comparison of the plots *v vs. T* obtained from measurements with and without initial $^{16}O_2$ in the gas mixture for a – $La_{0.5}Sr_{1.5}MnO_{3.99}$ and b – $La_{0.7}Sr_{0.3}MnO_{3.01}$

that becomes dominant in the absence of $^{18}O_2$. As a result, the $^{16}O^{18}O$ partial pressure passes through a maximum at ~870 K. Moreover, above 830 K, the coefficient increases due to the partial reduction of Mn^{4+} in the manganite lattices, so at high temperatures out-diffusion and partially heteromolecular ^{18}O exchange were predominating with all manganites.

In order to clarify the reason for the formation of $^{16}O^{18}O$ in the 2nd temperature range, all ^{18}O exchange experiments were repeated, but instead of $^{16}O_2$, $^{18}O_2$ and Ar, a gas mixture without $^{16}O_2$ was introduced into the reaction vessel before heating. Theoretically, homomolecular ^{18}O exchange can be excluded, if no $^{16}O_2$ is available in the gas phase. Unfortunately, with all manganites small quantities of $^{16}O_2$ are formed by completely heteromolecular exchange in the 1st temperature range, already. The resulting partial pressure of $^{16}O_2$, however, is much smaller than in the case of equimolar initial quantities of $^{16}O_2$:$^{18}O_2$. Therefore, the homomoleculear ^{18}O exchange rate without initial $^{16}O_2$ in the gas phase should be significantly lower than that observed during the standard ^{18}O ex-

change measurements. The contribution of the homomolecular exchange to the formation of $^{16}O^{18}O$ can be estimated from the temperature-dependent variation of v (Eq. (7)).

This coefficient is much more sensitive to homomolecular than to partially heteromolecular exchange [13, 14] and it is normalized to its initial value, thus allowing semi-quantitative kinetic conclusions from polythermal measurements. For $La_{0.5}Sr_{1.5}MnO_{3.99}$ (Fig. 3a), the plots of v *vs.* T with and without initial $^{16}O_2$ in the gas phase are absolutely identical. That means that the formation rate of $^{16}O^{18}O$ is independent of the $^{16}O_2$ partial pressure, as in the case of partially heteromolecular ^{18}O exchange (Eq. (2a)). Hence, it is evident for $La_{0.5}Sr_{1.5}MnO_{3.99}$ that $^{16}O^{18}O$ is formed by partially heteromolecular exchange, only. For the $AMnO_3$ (A=La, Sr) compounds, however, the slope of v *vs.* T is identical in the 2nd temperature range, only (Fig. 3b). Here, the formation rate of $^{16}O^{18}O$ is independent of the $^{16}O_2$ concentration, too, clearly suggesting that $^{16}O^{18}O$ is formed by partially heteromolecular exchange in the 2nd temperature range. At higher temperatures, the graphs separate and for all $AMnO_3$ compounds, the slope of v *vs.* T is higher if initial $^{16}O_2$ was available in the gas mixture. This is due to the occurrence of homomolecular ^{18}O exchange in the 3rd temperature range as has already been concluded from the standard measurements. The separation of the graphs confirms the accuracy of the initial assumption that the homomolecular ^{18}O exchange rate decreases if no initial $^{16}O_2$ is available in the gas phase.

Comparing the four manganites with different structure and Mn^{3+}/Mn^{4+} ratio, it can be seen that all types of ^{18}O exchange processes and out-diffusion take place on the manganites (Table 2).

Table 2 General order of ^{18}O isotope exchange and diffusion processes for manganites with different structure and Z_{Mn}

Composition	Temperature range/K			
	Completely heteromolecular exchange	Completely and partially heteromolecular exchange	Homomolecular completely and partially heteromolecular exchange	Partially heteromolecular exchange and out-diffusion
$LaMnO_{3.10}$	535–575	575–725	725–830	>830
$La_{0.7}Sr_{0.3}MnO_{3.01}$	520–550	550–630	630–775	>835
$La_{0.5}Sr_{1.5}MnO_{3.99}$	665–695	>695	no homomolecular	>675 K[1]
$SrMnO_{2.96}$	575–605	605–665	665–765	>840

[1]Here, completely and partially heteromolecular ^{18}O exchange take place

The general order of processes is similar for all compounds:

T_1–T_2 → completely heteromolecular ^{18}O exchange only
T_2–T_3 → completely and partially heteromolecular ^{18}O exchange
T_3–T_4 → homomolecular and both heteromolecular ^{18}O exchange reactions
T_4–T_5 → out-diffusion and partially heteromolecular ^{18}O exchange

The K_2NiF_4-like structure showed the lowest ^{18}O exchange activity and $La_{0.5}Sr_{1.5}MnO_{3.99}$ did not catalyse the homomolecular ^{18}O exchange (Table 2). Rather low onset temperatures were observed for perovskites with a minimum of T_{on} of for $La_{0.7}Sr_{0.3}MnO_{3.01}$. Onset-temperatures of less than 550 K for completely and less than 700 K for the homomolecular ^{18}O exchange are typical for good oxidation catalysts [7, 24] and make the $AMnO_3$ compounds prepared by freeze-drying attractive for further catalytic studies. The fact that $La_{0.7}Sr_{0.3}MnO_{3.01}$ exhibits the highest ^{18}O exchange activity is remarkable, since a very low quantity of cation and anion vacancies is available in this compound.

Although there is no real excess oxygen in the manganite structures (see above), the high oxidation potential of Mn^{4+} in the manganite structures led to a slight out-diffusion at elevated temperatures (T>675 K). The most pronounced reduction of Mn^{4+} to Mn^{3+} – indicated by the largest increase of s – was observed with $LaMnO_{3.10}$. This can be explained by the fact that – in spite of the lowest average oxidation state of Mn (Z_{Mn}=3.20) – $LaMnO_{3.10}$ is the only phase with a numerical excess of oxygen. Although Z_{Mn} is considerably higher for the other compounds (Table 1), the rate of the Mn^{4+} reduction is very slow. Remarkably, the onset temperature of out-diffusion from the K_2NiF_4-like $La_{0.5}Sr_{1.5}MnO_{3.99}$ was more than 150 K lower than that for the $AMnO_3$ compounds. This behaviour can be explained by means of the bond-valence method [19]. The strength-values of oxygen chemical bonding calculated for $LaMnO_3$ (V~2.08) and $SrMnO_3$ (V~2.10) are very similar and differ significantly from those of $La_{0.5}Sr_{1.5}MnO_4$. In the K_2NiF_4-structure, two different oxygen sites can be distinguished. O(1) with V=1.75(3) is surrounded by one Mn^{z+} and five $La^{3+}(Sr^{2+})$ ions. The other oxygen anion, O(2) with V=2.37(3) is coordinated by two Mn^{z+} and four $La^{3+}(Sr^{2+})$ cations. According to these calculations, it is reasonable to assume that the bond strength of O(1) in the K_2NiF_4-structure is lower than that of the O anions in the $AMnO_3$ compounds and lower than that of O(2). Hence, it can be understood, why the reduction of Mn^{4+} in $La_{0.5}Sr_{1.5}MnO_{3.99}$ starts at lower temperatures than with other manganites.

Conclusions

Manganites of different structure and average oxidation state of Mn exhibit a similar ^{18}O isotope exchange behaviour with four temperature ranges under the above measuring condition. In spite of the high oxidation potential of Mn^{4+}, only small amounts of $^{16}O_2$ are released from the solid manganites above 675 (K_2NiF_4-structure) and 830 K ($AMnO_3$ compounds), respectively. The low onset temperature of Mn^{4+} reduction in $La_{0.5}Sr_{1.5}MnO_{3.99}$ was explained by means of the bond-valence model. All types of ^{18}O exchange (homomolecular, partially and completely heteromolecular) were catalysed on the $AMnO_3$ compounds but not on $La_{0.5}Sr_{1.5}MnO_{3.99}$. The K_2NiF_4-structure is much less active than the other manganites, especially the perovskites. The highest ^{18}O exchange activity was observed for $La_{0.7}Sr_{0.3}MnO_{3.01}$ with Z_{Mn}=3.32 and a lack of anion and cation vacancies in the structure. Obviously, the Mn^{3+}/Mn^{4+} ratio and the vacancy concentration in the bulk of the manganites are of minor importance

for the ^{18}O exchange behaviour. The rather low onset temperatures of the completely heteromolecular and the homomolecular exchange make the perovskites attractive for further, detailed catalytic studies.

* * *

The financial support of the Deutscher Akademischer Austauschdienst (DAAD), the Deutsche Forschungsgemeinschaft (DFG) and the Ministry of Science and Technology of Russian Federation (grants RUS 139/97) is gratefully acknowledged.

References

1 R. A. De Souza and J. A. Kilner, Solid State Ionics, 106 (1998) 175.
2 R. von Helmot, J. Wecker, B. Holzapfel, L. Schultz and K. Samwer, Phys. Rev. Lett., 71 (1993) 2331.
3 Y. Moritomo, A. Asamitsu, H. Kawahara and Y. Tokura, Nature, 380 (1996) 141.
4 L. G. Tejuca and J. L. G. Fierro, Adv. Catal., 36 (1989) 237.
5 N. Guilhaume and M. Primet, J. Catal., 165 (1997) 197.
6 D. W. Johnson, P. K. Gallagher, F. Schrey and W. W. Rhodes, Ceram. Bull., 55 (1976) 520.
7 L. Marchetti and L. Forni, Appl. Catal. B, 15 (1998) 179.
8 L. Lisi, G. Bagnasco, P. Ciambelli, S. de Rossi, P. Porta, G. Russo and M. Turco, J. Solid State Chem., 146 (1999) 176.
9 P. Salomonsson, T. Griffin and Bengt Kasemo, Appl. Catal. A, 104 (1993) 175.
10 L. A. Sazonov, Z. V. Moskvina and E. V. Artamonov, Kinet. Catal., 15 (1974) 100.
11 J. A. Kilner, R. A. De Souza and I. C. Fullarton, Solid State Ionics, 86–88 (1996) 703.
12 L. V. Borovskikh, G. N. Mazo and V. M. Ivanov, Vestnik Mosk. Univ., Khimiya, 40 (1999) 373.
13 E. Kemnitz, A. A. Galkin, T. Olesch, S. Scheurell, A. P. Mozhaev and G. N Mazo, J. Thermal Anal., 48 (1997) 997.
14 A. A. Galkin, G. N. Mazo, V. V. Lounin, S. Scheurell and E. Kemnitz, Rus. J. Phys. Chem., 72 (1998) 1459.
15 V. S. Musikantov, V. V. Popovski and G. K. Boreskov, Kinet. Catal., 5 (1964) 624.
16 G. K. Boreskov, Adv. Catal., 15 (1964) 285.
17 V. S. Musikantov, G. I. Panov and G. K. Boreskov, Kinet. Catal., 10 (1969) 1047.
18 V. S. Musikantov, G. I. Panov and G. K. Boreskov, Kinet. Catal., 14 (1973) 948.
19 D. Brown and D. Altermatt, Acta Cryst. B41 (1985) 244.
20 J. F. Mitchell, D. N. Argyriou, C. D. Potter, D. G. Hinks, J. D. Jorgensen and S. D. Bader, Phys. Rev. B, 54 (1996) 6172.
21 C. Ritter, M. R. Ibarra, J. M. De Teresa, P. A. Algarabel, C. Marquina, J. Blasco, J. Garcia, S. Oseroff and S.-W. Cheong, Phys. Rev. B, 56 (1997) 8902.
22 J. Toepfer and J. B. Goodenough, J. Solid State Chem., 130 (1997) 117.
23 M. Hervieu, R. Mahesh, N. Rangavittal and C. N. R. Rao, Eur. J. Solid State Inorg. Chem., 32 (1995) 79.
24 C. Doornkamp, M. Clement, X. Gao, G. Deo, I. E. Wachs and V. Ponec, J. Catal., 185 (1999) 415.